RSC Advances

ROYAL SOCIETY OF CHEMISTRY

www.rsc.org/advances

Evolution of excitation wavelength dependent photoluminescence in nano CeO_2 dispersed Ferroelectric Liquid Crystals

Puja Goel[1], Manju Arora[2], A. M. Biradar[2]

[1]Division of Agricultural Chemicals, Indian Agricultural Research Institute, New Delhi 110012, India

[2]Liquid Crystal Group, CSIR- National Physical Laboratory, Dr. K. S. Krishnan Marg, New Delhi 110012, India

Email: pujagoel@gmail.com

Optical properties of nano Ceria (CeO_2) dispersed ferroelectric liquid crystals (FLCs) have been investigated by excitation wavelength dependent photoluminescence (PL) spectroscopy. PL spectra of nano Ceria exhibit strong excitation wavelength dependence in 255 – 370 nm range. The red shift in violet emission band of Ceria i.e. from 368 nm to 396 nm with increasing excitation wavelength has been attributed to recombination of electrons trapped in the defect band and deeply trapped holes in oxygen vacancies. This excitation wavelength dependence of Ceria has been markedly manifested in the PL response of FLC/CeO_2 nanocomposites as well. PL emission recorded at an excitation wavelength where host and guest materials shows intense emission, i.e. 340 nm, exhibits a quenching effect which is connected to the overlapping of emission and absorption bands of host FLC and guest Ceria NPs respectively. No blue/red shift in the spectral energy band was observed at 310 and 340nm excitations. On the other hand, emission spectra at lower excitation wavelength follows reverse trend: enhancement in the emission intensity with a large blue shift in spectral energy band. The mechanisms involved in the changes of the PL spectrum of FLC/Ceria nanocomposites with variable ceria concentration and excitation wavelengths are discussed in detail.

Introduction

The potential applications of ferroelectric liquid crystals (FLCs) in optical storage devices, flat panel displays, luminescent liquid crystal displays, spatial light modulators and electro-optic memories has led a great deal of research over the past few decades owing to their bistability and faster switching response in comparison to conventionally used nematic liquid crystals. The use of nanomaterials, quantum dots etc. in liquid crystal (LC) science has further revived the hopes of researchers who have been looking for the performance enhancement as well as finding new application prospective of FLCs based devices. Dispersing an appropriate amount of nanomaterials in FLCs not only enhances the physical properties of host FLCs but also can impart novel phenomenon in nanocolloids/ nanocomposites. In addition to this, nanomaterials and quantum dots have also played an important role in bringing forward LC materials for application in luminescent display devices[1-4]. In general, LC displays have comparatively low brightness and energy efficiency due to the use of polarizers and absorbing colored filters in their construction. They mostly fluoresce in the blue region of visible spectrum as a broad emission band which is the main limitation in the development of full-color emissive LC display. Since a display device requires blue, green and red emitting liquid crystalline matrices without overlapping their emission bands, for improving the color performance of LCs, luminescent LC materials are found to be promising for fabricating emissive type displays. To achieve this, the sheets of photoluminescent material in LCs have been used as an active color filter. However, new research trends revolves around to find out the application potential of nanomaterials/ Quantum dots for imparting photoluminescence (PL) in LC materials taking into consideration the preliminary results reported so far[1-6]. For ex. (a) Gold nanoparticles (NPs) were found to increase the PL emission intensity of deformed helix FLC materials by nine folds[1] (b) emission

profile of Nematic LCs were strongly influenced in presence of Dye molecules[5] (c) enhancement and quenching of PL has also been reported for silver NPs doped LCs[6]. In addition to this, the rare earth materials containing liquid crystals also follows guest-host effect for optimizing the luminescent and liquid crystalline properties of the system independently[7]. The rare earth ions exist mostly in trivalent state and form three types of complexes depending upon metal-to-ligand ratio: (i) tris-complexes, (ii) Lewis base adducts of tris-complexes and (iii) tetrakis complexes. Rare earth oxide Ceria (CeO_2) is a wide energy band gap semiconductor (Eg ~ 5.5 eV) with a fluorite structure and has attracted great deal of attention for its tunable electronic and optical characteristics[8]. It is extensively considered in the field of luminescence, semiconductor devices, fuel cells and solar cells due to its chemical stability, high oxygen storage capacity and easily shifting between Ce^{4+} and Ce^{3+} oxidation states[8-10]. Owing to these remarkable features, we have dispersed nano Ceria in FLCs and characterized their photoluminescence response in terms of varying ceria concentration and wavelength of PL excitation.

Experimental

Suspension of Ceria NPs (Sigma Aldrich) was obtained by dispersing NPs in millipore water (1:100) followed by one hour ultrasonication. Selective amounts of this suspension (0.5, 1 and 5 µl) were added to fixed amount of FLC material (3mg) at 25 ± 2^0C in order to obtain FLC-Ceria nanocomposites. These mixtures were heated at 120 ^{0}C for 10 minutes followed by rigorous mixing. This heating and mixing process was repeated thrice in order to ensure complete removal of water content. Mixtures were cooled to the room temperature (25 ± 2^0C) and placed on one of the opening of electro-optic cells. Cells were then kept in an oven at a 120^0C temperature (which is slightly above the nematic to isotropic transition temperature of FLC

material i.e. 114.5 ^{0}C) for 20 minutes so that material flows inside the cell through capillary action. Samples were slowly cooled inside the oven and taken out when oven temperature reaches 25±2^{0}C.

Electro-optic cells for textural and optical investigation were fabricated by etching a square patterned electrode on ITO (resistivity ~30 Ω/) coated glass substrate using photolithography technique. Cell thickness of ~4 μm was maintained using Mylar spacers. The phase sequence of investigated FLC, i.e., KCFLC 7s is as follows:

where Cryst., SmC*, SmA, N*, and Iso., represent crystal, chiral smectic C, smectic A, chiral nematic, and isotropic phases, respectively. For characterization of ceria NPs, High Resolution Transmission Electron Microscopy (HRTEM) was performed using the Tecnai G2F30 S-Twin (FEI; Super Twin lens with C s 1.2 mm) instrument having a point resolution of 0.2 nm and a lattice resolution of 0.14 nm. The samples for HRTEM analysis was prepared by dispersing the ceria NPs in acetone through ultrasonication and drying a droplet of the dispersion on a carbon coated copper grid at room temperature (25±2^{0}C). High-resolution polarizing optical microscope (POM, Carl Zeiss, Axioskop-40, Germany) equipped with computer controlled charge coupled device (CCD) camera was used to investigate the optical textures of pure and FLC- ceria NPs dispersions. Photoluminescence spectra of pure and ceria dispersed samples were recorded using a Fluorolog (Jobin Yvon – Horiba, model-3-11) spectrofluorometer. To record the UV–Vis absorption spectrum of pure materials as well nanocomposites in 200nm -800nm range , we have used Shimadzu UV–Vis spectrophotometer (model No. UV-2401 PV).

Results and Discussion

HRTEM micrographs in Fig 1(a) revealed that octahedral shaped ceria NPs have an average size of ~18.5 nm with a very narrow size distribution. Size distribution of nanoparticles can also be seen through the histogram derived from the TEM picture of ceria NPs (Figure 1 (b)). Distribution can be well fitted by the log normal distribution function [11]

$$y = y0 + \frac{A}{w \times x\sqrt{2\pi}} \exp\left(-\frac{(\ln(x/xc))^2}{2 \times w^2}\right)$$

where "w" represents the standard deviation and "x_c" is the mean particle size.

In Figure 1(c), the image of a single octahedron clearly shows that edges are sharp and lattice plane are well aligned. Further, to look in to the textural changes in FLC material in presence of secondary phase ceria NPs, Bright (B) and scattered (S) state of pure and dispersed NPs samples were analyzed by recording high resolution optical micrographs under a crossed polarizer. It is evident from Figure 2 that homogenous alignment is retained up to 5 µl Ceria NPs addition and the NPs were uniformly dispersed within the FLC material.

So far, reports pertaining to the PL evolution in FLC based composites are predominantly focused on the PL intensity variations with dopant addition. In these investigations, our focus is to understand the mechanism of the excitation energy dependent PL emission (since dopant exhibits strong excitation dependence) in terms of the change in local field and coupling between the excitons of ceria nanoparticles and FLC molecules.

PL spectra of the pure FLC and ceria nanoparticles were recorded at different excitation wavelengths in the range from 255 nm – 370 nm. In Fig. 3 (a), PL spectra of pure FLC shows broad absorption in the region 325 nm to 575 nm with peak maxima at ~ 396 nm and weak submerged components. Submerged components present in the broad asymmetric PL emission of

pure FLC at ~ 396 nm were determined by using Gaussian fitting. As shown in Fig. 3(b) three discrete submerged components with maxima at 380 nm, 412 nm and 446 nm could be resolved. The bands at 380 nm, 412 nm and 446 nm appear due to luminance of the trans-isomers (π, π^*), cis-isomers (n, π^*) transitions and the intermediate conformation of excited *trans* isomers respectively [12-14]. Further, it can be seen that the intensity of PL emission signal increases from 250 nm to 340 nm excitation wavelength range and then reduces drastically on further increasing excitation wavelength to 370 nm. The peak ~ 396 nm (ultraviolet emission) with submerged components in FLC is ascribed to the radiative relaxation of electrons from the lowest energy unoccupied molecular orbital (LUMO) to the highest energy occupied molecular orbital (HOMO) levels in FLC. Uniform surface morphology with minor surface defects in FLC leads to the enhancement of PL signal upto 340 nm excitation. Whereas, drastic reduction in signal intensity at 370 nm excitation is attributed to the distortion in the layer/helical structure and formation of topological defects in the host FLC material [15] which leads to the saturation of energy levels and thereby negligible energy absorption. As we know that chiral liquid crystals can form self-assembled photonic band gap structures, which can be tuned by external fields. Such structures are realized in the helical cholesteric, the cholesteric blue, the helical ferroelectric and the smectic blue phases. Photonic band gap materials are characterized by the property that classical light propagation in them is forbidden for some range of frequencies because the density of photon states is suppressed in the stop band and is enhanced at the band edges. This may be the reason for drastic reduction in the intensity of PL emission at 370 nm which we considered as the distortions in the layer/helical like structure and defects formation in the host lattice that act as stop band [16].

On contrary to this, PL spectra of pure ceria nanoparticles recorded at different excitation wavelengths (Fig. 4) exhibit a shift in PL maxima to higher wavelengths (red shift) with a broad emission peak. The emission bands originating from the ligand-to-metal charge transfer states $O \rightarrow Ce^{4+}$ (LMCT) from O_2^{2-} ligand to Ce^{4+} ions via hopping of electrons[17] in the range >3 eV and from the defect levels localized between Ce_{4f} band and O_{2p} band are the basic reason for broader emission peak. In CeO_2, Ce_{4f} level with a width of 1eV is localized at the forbidden gap (~ 5.5 eV), which lies at 3 eV over the valence band (O_{2p})[8]. As shown in Fig. 4, the violet broad emission with peak maxima in the range from 365 to 400 nm are observed by the excitation wavelengths (255 – 370 nm) even below the band gap (~5.5 eV) energy of ceria. These emissions are assigned to the electronic transition between valence band to Ce_{4f} level. The red shift of emission peak i.e. from 368 to 396 nm with increasing excitation wavelengths are attributed to recombination of electrons trapped in the defect band and deeply trapped holes in oxygen vacancies. In addition to that, the emission intensities shows nonlinear behavior: first increasing, reaching maximum at 340 nm and finally decreasing with negligible emission at 370 nm excitation energies respectively. The rate of the recombination between photogenerated holes and electrons might be reduced on increasing the excitation wavelength above 340 nm which leads to the complete quenching of PL signal in ceria nanoparticles.[18,19]

Further, to understand the mechanism of excitation wavelength dependent PL peak position and intensity of FLC/Ceria nanocomposites, PL spectra were recorded at 255nm, 280 nm, 310 nm and 340 nm excitations. In Figure 5 (a), the characteristics of the PL spectra (at 255nm excitation) of the nanocomposites were exactly similar to ceria NPs except the fact that intensity of PL signals changes with varying ceria concentration in FLC. The violet light emission at 255 nm excitation corresponds to the emission from electron transition between

Ce*4f*→O_{2p} and defects level→O_2. It can be noticed that PL signal enhances on increasing ceria nanoparticles concentration upto 1µl and then quenches on further increasing dopant concentration to 5 µl. At higher doping concentrations, NPs dispersed among the FLC will be situated relatively close together as compared to the lower doping concentration. When this happens, the probability of excitation energy transfer among the NPs will be increased which might serve as a path to the non-radiative decay resulting in a quenching of PL emission. Such concentration dependent quenching effect dominates if the energy migration takes places in the time necessary for the radiative decay.[20] Similar to the above, emission spectra at 280 nm (Fig.5 (b)) excitation also had the enhancement and quenching effect in nanocomposites with a large blue shift in the spectral energy band of host FLC. However, there is an additional peak (very feeble) appearing at 533 nm (λ_{ext} = 280 nm) which corresponds to the excimer luminescence[21]. There exhibits efficient interaction of FLC phenyl rings with ceria NPs via hydrogen bonding which may lead to the freezing of molecular motion and formation of predimer state which gives excimer PL[22] at 280 nm excitation.

In Figure 5 (c-d), PL spectra recorded at 310 nm and 340 nm excitations, strong and broad absorption signal with peak maximum at 396 nm is observed for pure FLC as well as ceria doped analogues. At these excitation wavelengths, 533 nm signal (i.e. excimer PL) is absent which might be due to the instability of predimer states at higher excitation wavelengths. The PL spectra exhibit quenching and enhancement of emission signal with varying dopant concentration. In 0.5 µl ceria NPs dispersed samples, the intensity of the 396 nm emission band was much lower, indicating a quenching of PL emissions. This quenching in emission is attributed to the alteration of defect bands of ceria in FLC matrix and overlapping of emission and absorption band of host FLC and guest ceria NPs. To get a clear understanding of the

mechanism playing a role in modifying PL emission of nano ceria dispersed system, UV-Vis absorption spectra of pure FLC, Ceria NPs and all the nanocomposites were recorded in 200-800nm range and presented in Figure 6. One can notice a visible change in the absorption features of FLC-Ceria nanocomposites in 280 -340 nm range. These features are assigned to the absorption occurring due to the alteration in the defect levels of ceria NPs after dispersing in FLC media. Figure 7a shows the overlapping of absorption and emission band of FLC and Ceria NPs. Schematic diagram depicting the position of energy bands of FLC and Ceria NPs is also presented in Figure 7 b. Enhancement in PL signal could be noticed on further increasing the ceria concentration upto 5 µl in these cases. The increase in emission of PL spectra can be attributed to the local field enhancement arising from the resonant coupling between the excitons of ceria NPs and FLC molecules as well as increase in the radiative recombination rate.

Conclusions

The enhancement and quenching in the PL intensity and enormous shift in the spectral energy band of nano ceria doped FLC nanocomposites have been demonstrated with varying excitation wavelength and ceria concentration. PL spectra of ceria NPs exhibit atypical excitation wavelength dependence which has been markedly imparted to the host material as well. Spectra recorded at an excitation wavelength where host liquid crystal and dispersed nanoparticle shows intense absorption, i.e. 340 nm, exhibits a quenching effect at lower doping concentration of NPs without any blue/red shift in band position. The quenching in emission intensity has been attributed to the overlapping of emission and absorption band of host FLC and guest nanoparticles and alteration of defect bands of ceria in FLC matrix. The emission spectra recorded at 255 and 280 nm excitation wavelengths follows reverse trend: large blue shift in the spectral energy band of host material and increase in the emission intensity at lower

concentration of NPs. These studies will provide important information in understanding, designing and tailoring PL properties of FLCs for futuristic display devices.

Acknowledgment

The authors sincerely thank Professor H S Gupta, Director IARI for continuous encouragement and interest in this work. One of the authors (P.G.) is also thankful to DST, New Delhi for financial support under INSPIRE Faculty Scheme (**IFA12-PH-38**) and SR/WOS-A/PS-68/2011.

References

[1]A. Kumar, J. Prakash, D. S. Mehta, A. M. Biradar, and W. Haase, *Appl. Phys. Lett,* 2009. **95**, 023117.

[2]W. A. Crossland, I. D. Springle, R. D. King, P. A. Bayley, A. B. Davey, and B. Needham, *Proc. SPIE*, 2002, **3955**, 70.

[3]L. J. Yu and M. M. Labes, *Appl. Phys. Lett*., 1977, **31**, 719.

[4]C. Weder, C. Sarwa, A. Montali, C. Bastiaansen, and P. Smith, *Science*, 1998, **279**, 835.

[5]V. Gayvoronsky, S. Yakunin, V. Pergamenshchik, V. Nazarenko, K. Paleweska, J Sworakowski, A. Podhorodecki, and J. Misiewicz, *Ukr. J. Phys. Opt.,* 2006, **7**, 116.

[6]S. Y. Huang, C. C. Peng, L. W. Tu, and C. T. Kuo, *Mol. Cryst. Liq. Cryst*., 2009, **507**, 301.

[7]A. Trovarelli, *Catalysis Reviews: Science and Engineering*, 1996, **38**, 439.

[8]C. Chunlin, Y. Shaoyan, L. Zhikai, L. Meiyong, and C. Nuofu, *Chinese Sci. Bull*., 2003, **48**, 1198.

[9]N. Shehata , K. Meehan M. Hudait, and N. Jain, *J. Nanopart. Res.,* 2012, **14**, 1173.

[10]S. Deshpande, S. Patil, S. Kuchibhatla, and S. Seal, *Appl. Phys. Lett.,* 2005, **87**, 133113.

[11]P.Goel, N. Viajayan and A. M. Biradar, *Ceram. Int.* 2012*,* 38, 3047.

[12]B. Liu, X.-L. Hu, J. Liu, Y.-D. Zhao, and Z.-L. Huang, *Tetrahedron Lett.* 2007*,* 48, 5958.

[13]B.-L. Lee and T. Yamamoto, *Polymer,* 2002*,* 43, 4531.

[14]M. P. Aldred, A. J. Eastwood, S. P. Kitney, G. J. Richards, P. Vlachos, S.M. Kelly, and M. O'Neill, *Liq. Cryst.,* 2005*,* 32, 1251.

[15]D.P. Singh, S.K. Gupta and R. Manohar, Advances in Condensed Matter Physics , Volume 2013, Article ID 250301

[16]P. P. Muhoray, W. Cao, M. Moreira, B. Taheri and A. Munoz, *Phil. Trans. R. Soc. A,* 2006, 364, doi: 10.1098/rsta.2006.1851.

[17]E.C.C. Souza, H.F. Brito and E.N.S. Muccillo, *J. Alloy. And Comp*., 2010, 491, 450.

[18]A. Kar, S. Kundu, and A. Patra, *J. Phys. Chem. C*, 2011, **115**, 118.

[19]A. T. de Figueiredo, V. M. Longo, S. de Lazaro et al., *J. Lumin*. 2007, **126**, 403.

[20]F. Benza, and H. P. Strunk, *AIP Adv.,* 2012**, 2**, 042115.

[21]M. Pope, and C. E. Swenberg, Electronic Processes in Organic Crystals, Clarendon, Oxford, 1982, Mir, Moscow, **Vol. 1** (1985).

[22]Y. P. Piryatinskii, O. V. Yaroshchuk, L. A. Dolgov, T. V. Bidna, and D. Enke, *Optics and Spectroscopy*, 2004, **97**, 537.

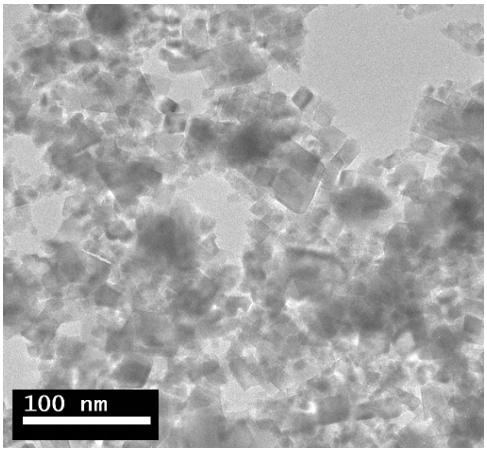

(a)

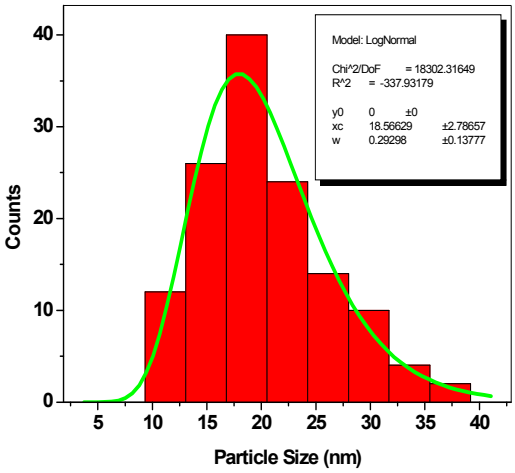

(b)

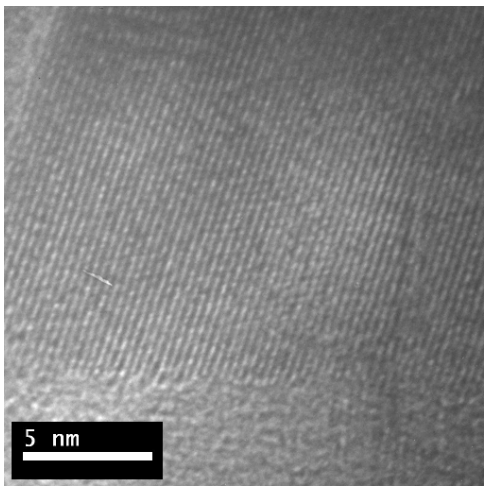

(c)

FIG. 1. High resolution transmission electron micrographs.(a) TEM images of the CeO_2 NPs (b) Particle size distribution histogram (w is standard deviation and xc represents mean particle size ~ 18.5 nm) (b)HRTEM image of CeO_2 NPs

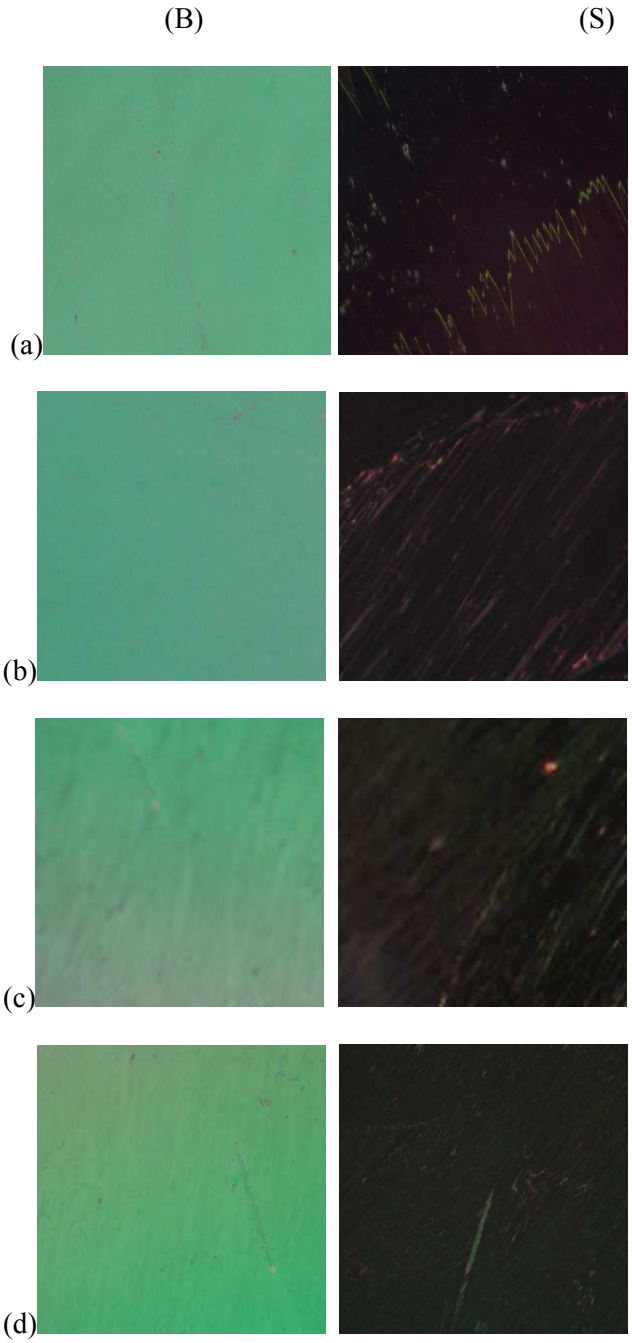

FIG. 2. Polarising optical micrographs of (a) FLC, (b) FLC-0.5% Ceria NPs, (c) FLC-1% Ceria NPs and (d) FLC-5% Ceria NPs. (B) and (S) denote 'bright' and 'scattered/dark' states respectively.

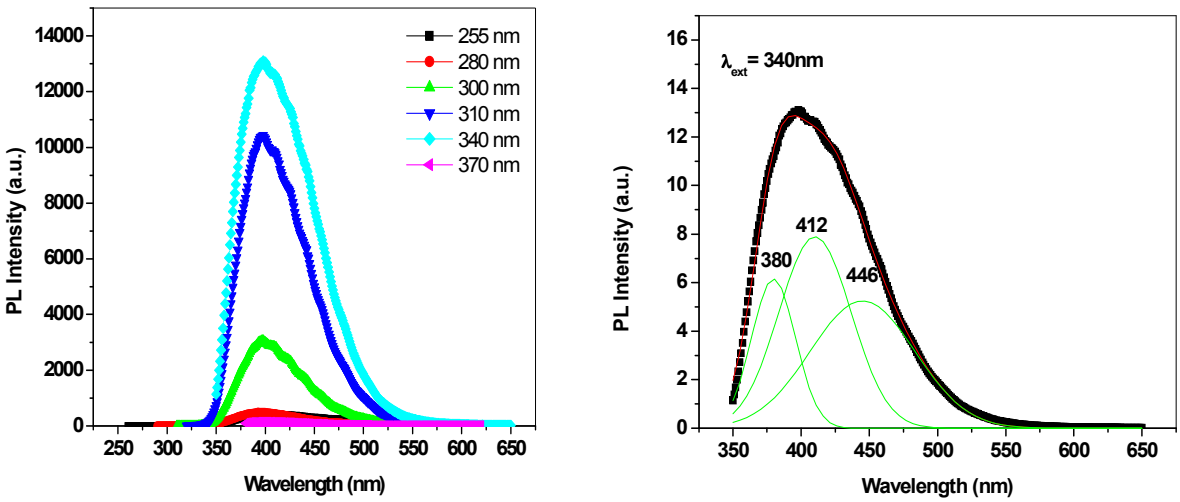

FIG. 3. (a) Emission plots for FLC material at different excitation wavelengths (b) The Gaussian fit for the PL peak at 396 nm shows three submerged components at 380, 412 and 446 nm

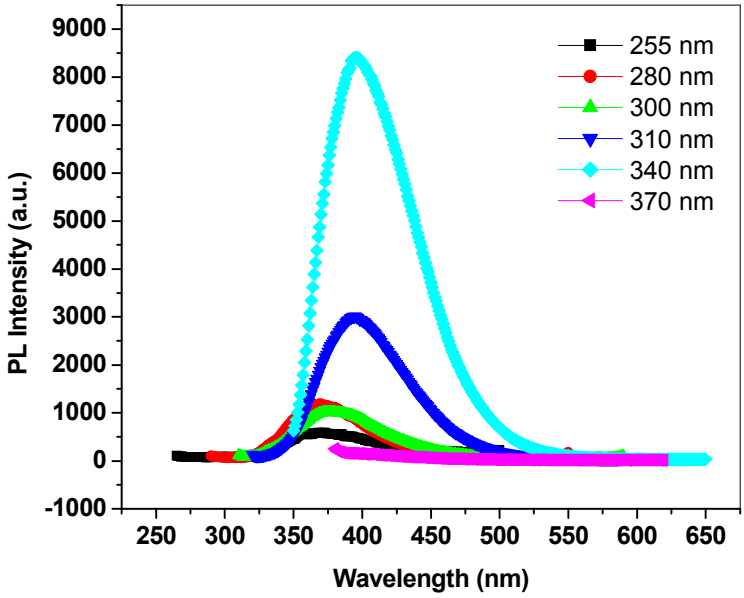

FIG. 4. Emission plots for ceria (CeO_2) NPs at different excitation wavelengths

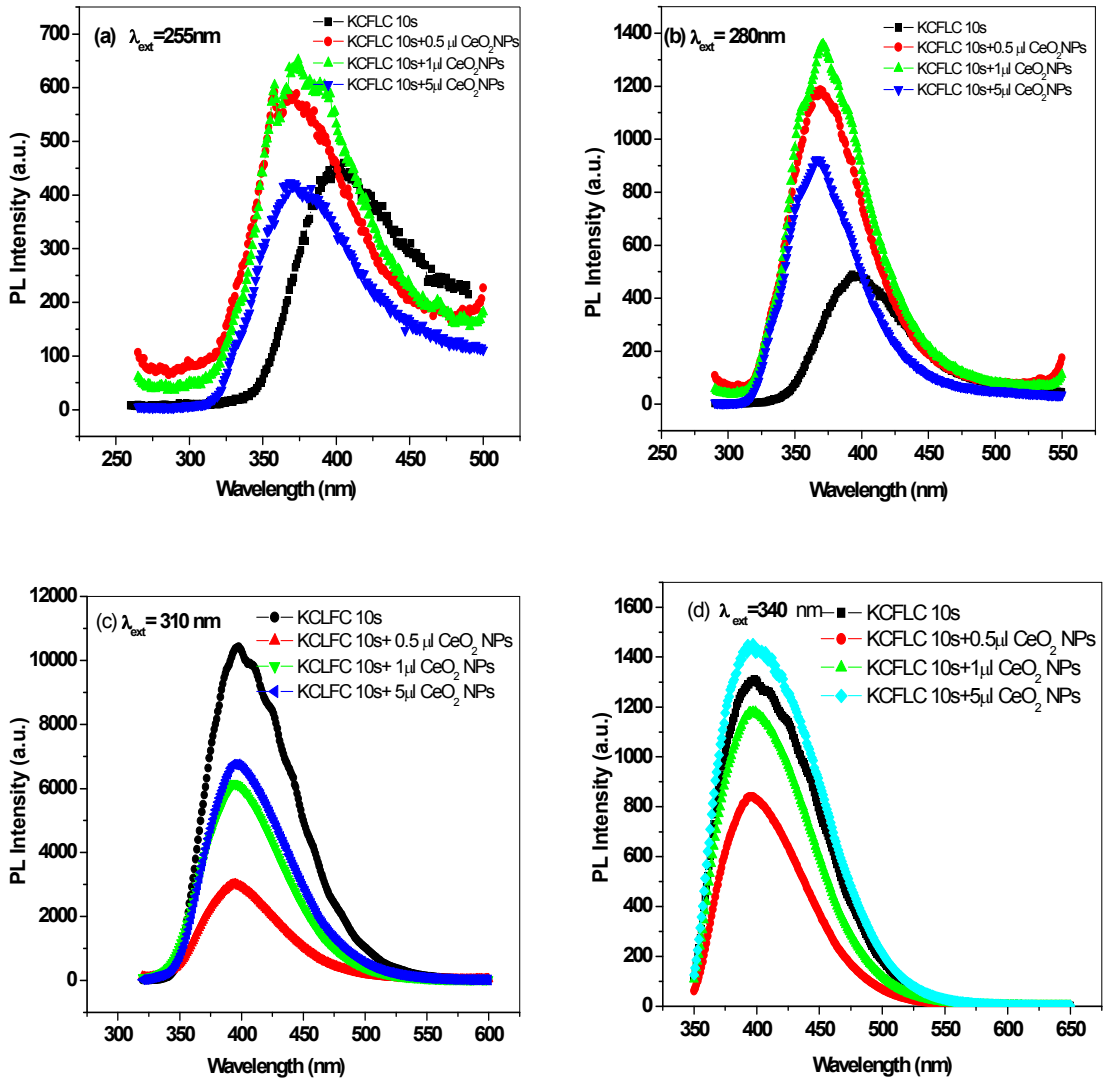

FIG. **5**. Emission plots for FLC pure and ceria NPs dispersed samples (a) $\lambda_{ext} = 280$ nm, (b) $\lambda_{ext} = 280$ nm, (c) $\lambda_{ext} = 310$ nm and (d) $\lambda_{ext} = 340$ nm

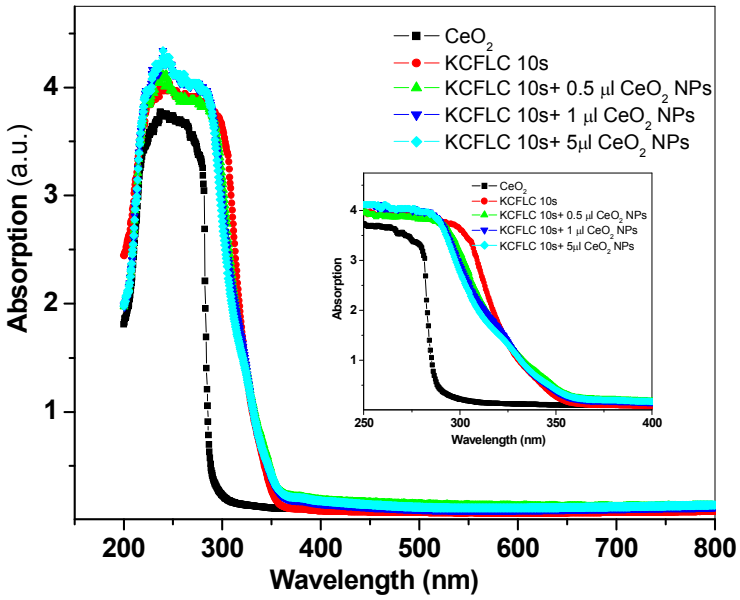

FIG. 6. UV-Vis Absorption Spectra of Ceria NPs, FLC pure and FLC-Ceria Nanocomposites

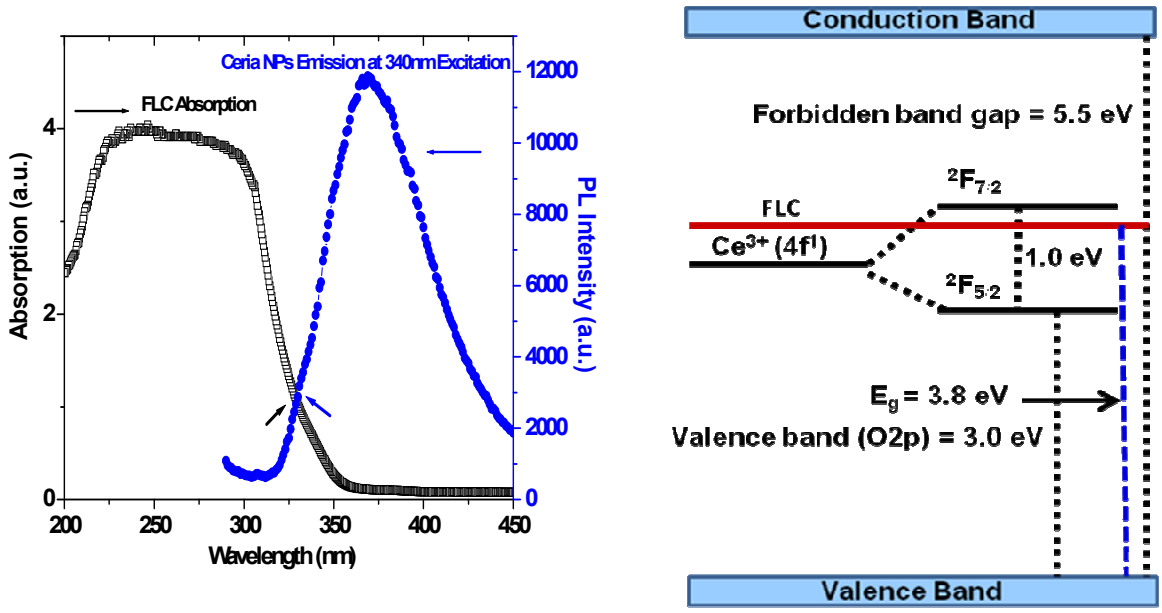

FIG 7 (a) Overlapping of absorption and emission band of FLC and Ceria NPs. (b) Schematic diagram depicting the tentative structure of band gap energy levels of FLC and CeO_2 NPs

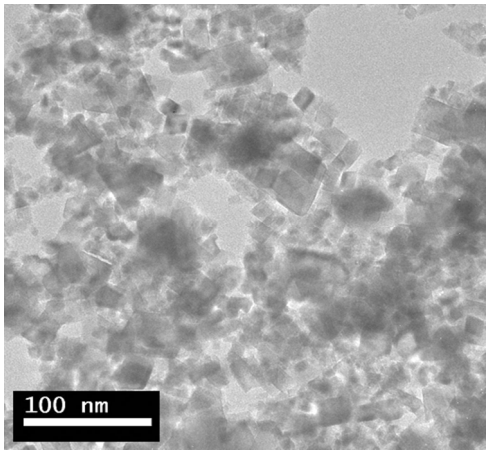

(a)

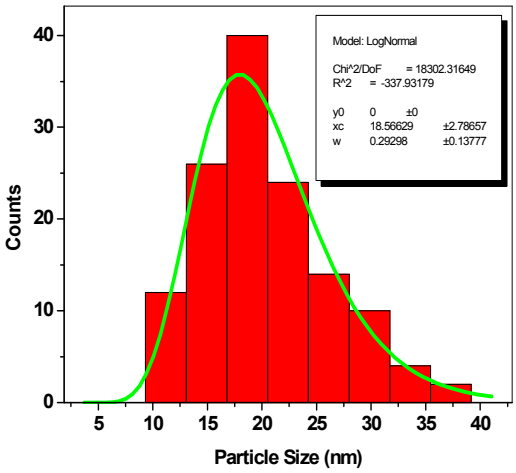

(b)

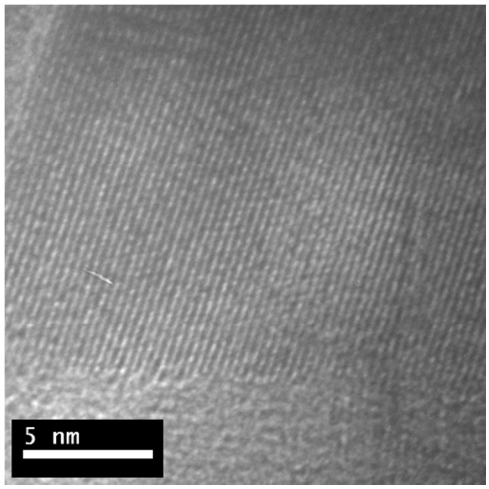

(c)

FIG. 1. High resolution transmission electron micrographs.(a) TEM images of the CeO_2 NPs (b) Particle size distribution histogram (w is standard deviation and xc represents mean particle size ~ 18.5 nm) (b)HRTEM image of CeO_2 NPs

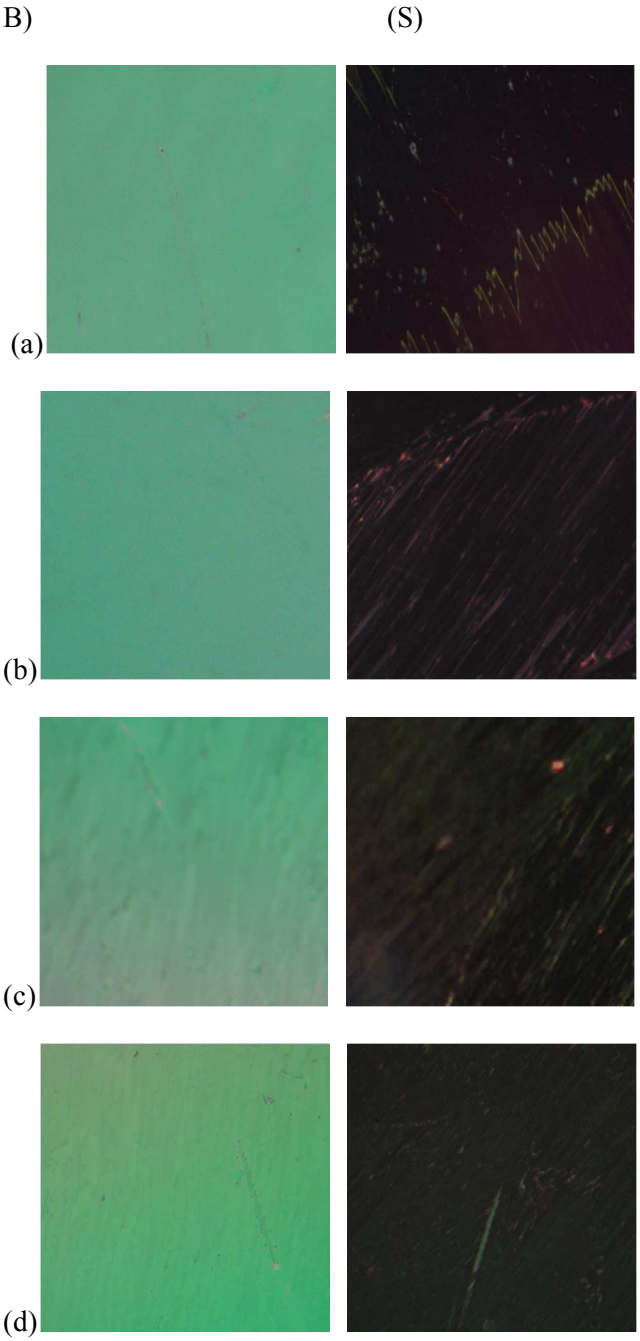

FIG. 2. Polarising optical micrographs of (a) FLC, (b) FLC-0.5% Ceria NPs, (c) FLC-1% Ceria NPs and (d) FLC-5% Ceria NPs. (B) and (S) denote 'bright' and 'scattered/dark' states respectively.

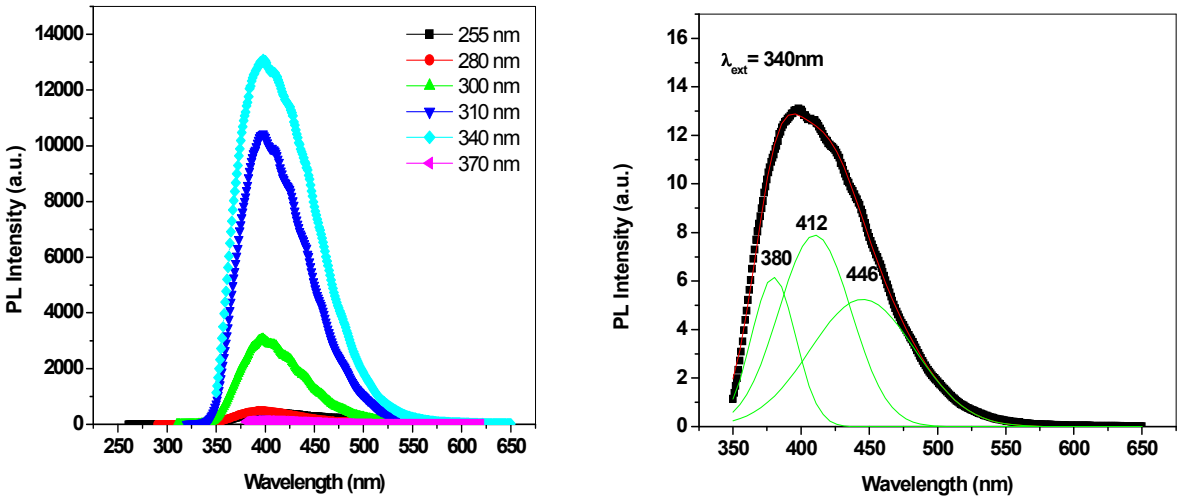

FIG. 3. (a) Emission plots for FLC material at different excitation wavelengths (b) The Gaussian fit for the PL peak at 396 nm shows three submerged components at 380, 412 and 446 nm

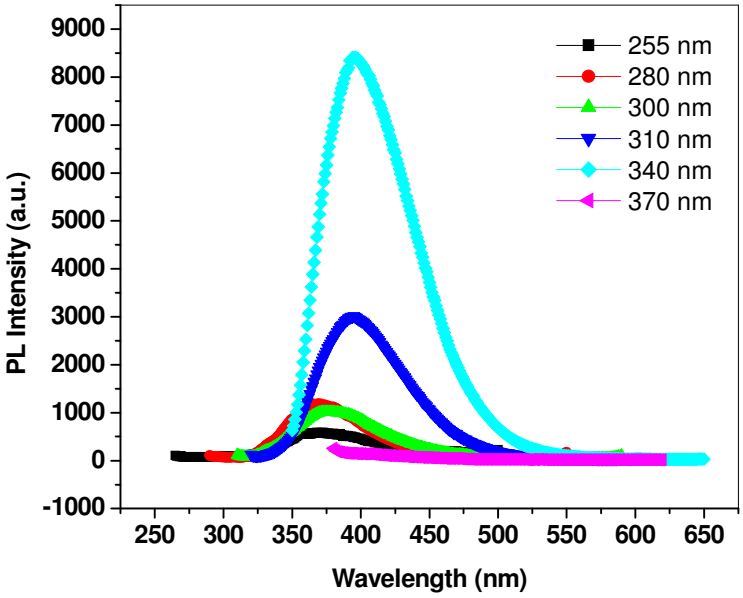

FIG. 4. Emission plots for ceria (CeO_2) NPs at different excitation wavelengths

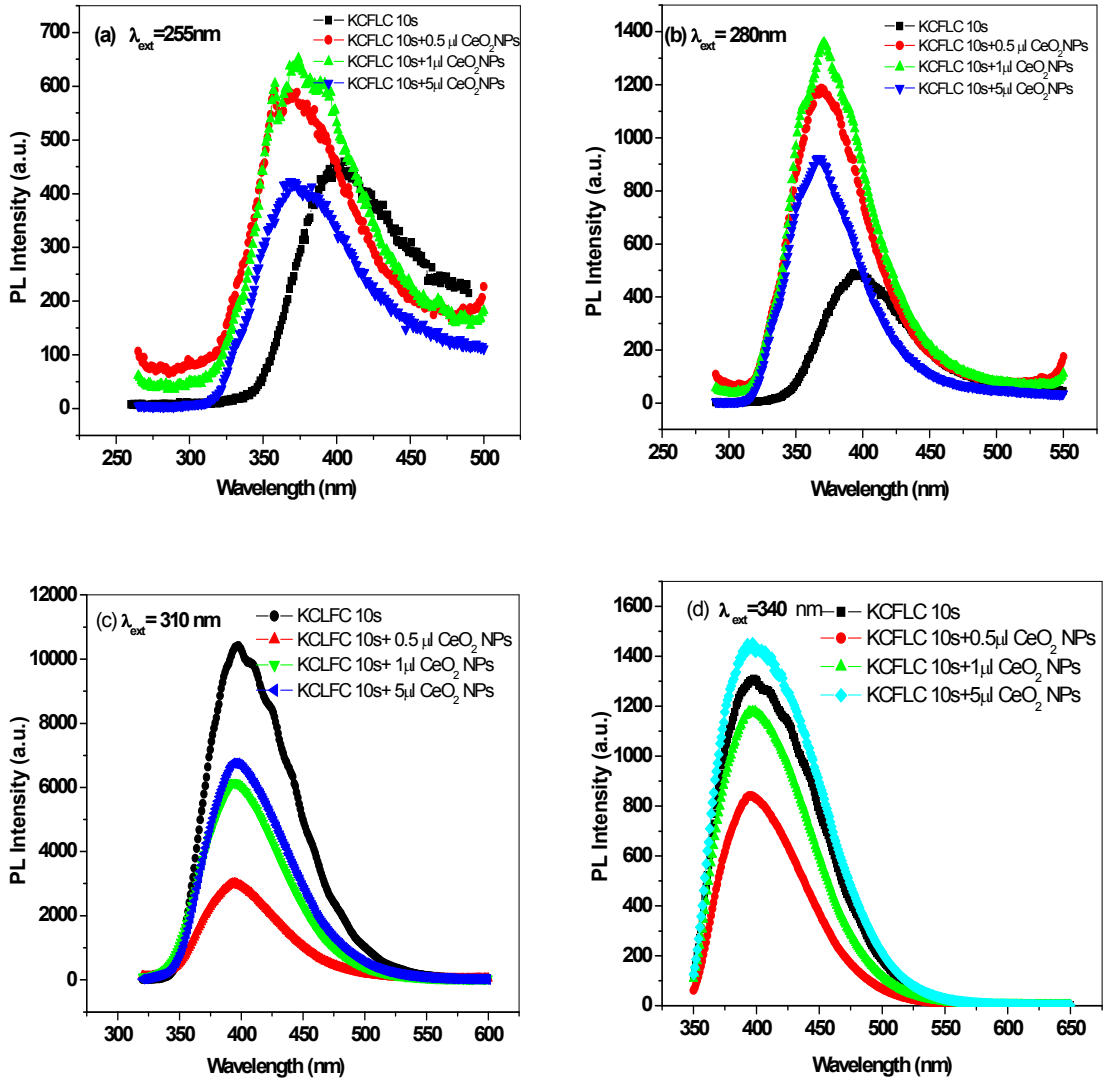

FIG. **5**. Emission plots for FLC pure and ceria NPs dispersed samples (a) λ_{ext} = 280 nm, (b) λ_{ext} = 280 nm, (c) λ_{ext} = 310 nm and (d) λ_{ext} = 340 nm

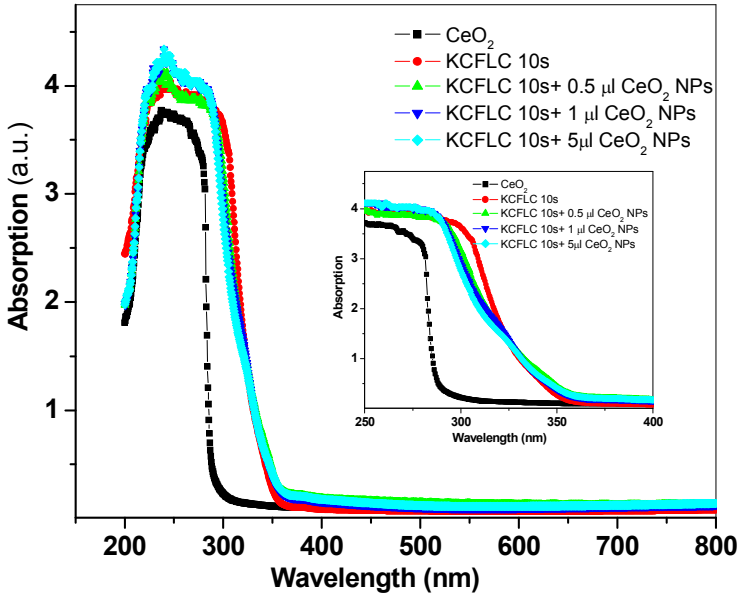

FIG. 6. UV-Vis Absorption Spectra of Ceria NPs, FLC pure and FLC-Ceria Nanocomposites

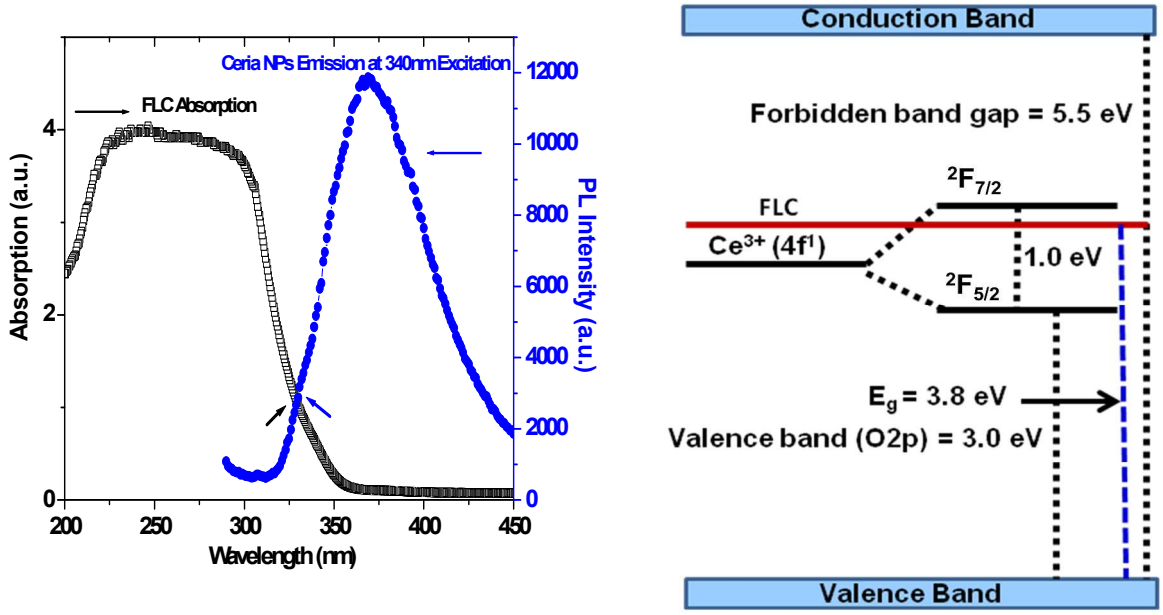

FIG 7 (a) Overlapping of absorption and emission band of FLC and Ceria NPs. (b) Schematic diagram depicting the tentative structure of band gap energy levels of FLC and CeO_2 NPs